Diaphragmatic Surface Reconstruction from Massive Temporal Registration of Orthogonal MRI Sequences

Leonardo I. Abe [*,1] **Marcos S. G. Tsuzuki** [*,2]
José Miguel M. Chirinos [*,3] **Thiago C. Martins** [*,4]
Toshiyuki Gotoh [**,5] **Seiichiro Kagei** [**,6] **Tae Iwasawa** [***,7]
Alexandre G. Silva [****,8] **Roberto S. U. Rosso Jr** [****,9]

Escola Politécnica da Universidade de São Paulo, Brazil.
Computational Geometry Laboratory
** *Yokohama National University, 79-1 Tokiwadai, Hodogaya-ku,*
Yokohama-shi, Kanagawa, 240-8501 Japan
*** *Kanagawa Cardiovascular Respiratory Center Kanazawa-ku,*
Yokohama-shi, Kanagawa, 236-0051 Japan
**** *Santa Catarina State University, Brazil*

Abstract: The diaphragm is an important component of the respiratory pumping process. Orthogonal temporal sequences of MR images are acquired in free breathing without use of contrast. The vertical intersection between two orthogonal temporal sequences is determined, the diaphragmatic level in the vertical segment is determined and used to perform the temporal registration. Previous works used similar temporal registration algorithms to reconstruct the diaphragmatic surface. However, it is shown that the available information was not efficiently used. The proposed method massively performs temporal registrations, and then validates the determined temporal registrations. The images to be used in the diaphragmatic surface reconstruction are determined and its associated diaphragmatic levels are collected. Positions with inconsistencies have their diaphragmatic level determined by interpolation. The proposed algorithm is tested with MR image sequences obtained from a healthy subject. *Copyright ©2014 IFAC.*

Keywords: Diaphragmatic surface reconstruction, temporal registration, MR imaging.

1. INTRODUCTION

The diaphragm is the main respiratory muscle and consequently is the major component to understand the respiratory mechanics. It is not possible to observe the diaphragmatic movement directly requiring the use of medical imaging devices. The lung movement has been studied using 4D CT during radiotherapy. However, because of ionizing radiation exposure, the use of repetitive 3D CT is not recommended to observe the lung movement. Thus, considering safety, MR devices are preferable.

Using MR temporal sequences, it was observed that COPD (Chronic Obstructive Pulmonary Disease) patients have paradoxical movements (Iwasawa et al., 2002), and that three motion patterns are enough to represent the internal structure lung movement within COPD patients (Gotoh et al., 2011). Cluzel et al. (2000) obtained a 3D MR

image in breath hold by shortening the exposure time for each image. However, it is known that the lung movement has hysteresis, and breath holding cannot capture the difference between inspiratory and expiratory movements.

In this work, free breathing temporal sequences of MR sagittal and coronal images without contrast are used, massive temporal registration is executed to perform the diaphragmatic surface reconstruction. It is shown that redundant information is present and inconsistent information can be filtered. This article is structured as follows. Section 2 explains some basic concepts and previous works on diaphragmatic surface reconstruction are presented. Section 3 explains the proposed algorithm with three steps: massive temporal registration, validation and surface reconstruction. Section 4 shows some results and Section 5 presents the conclusion.

2. BACKGROUND

A spatiotemporal volume (STV) $I(x, y, t)$ is defined by stacking the images from a temporal sequence, where x and y are pixel coordinates and t is time. A vertical plane $Q_s(x_s)$ is defined, such that it contains x_s. The intersection between $I(x, y, t)$ and $Q_s(x_s)$ defines a vertical 2D spatio–temporal (2DST) image where motion patterns generated

[1] e-mail: ishida.leonardo@gmail.com.
[2] e-mail: mtsuzuki@usp.br.
[3] e-mail: jmig.kat@gmail.com.
[4] e-mail: thiago@usp.br.
[5] e-mail: gotoh@ynu.ac.jp.
[6] e-mail: kagei@ynu.ac.jp.
[7] e-mail: tae_I_md@wb3.so-net.ne.jp.
[8] e-mail: alexandre.silva@udesc.br.
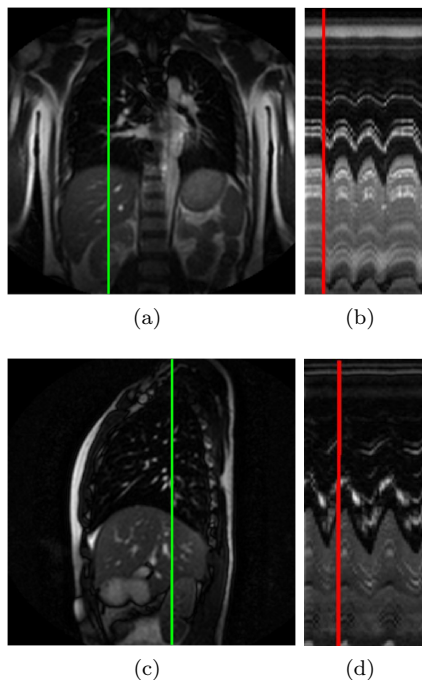[9] e-mail: rosso@udesc.br.

Fig. 1. (a) Coronal image with a vertical line at x_c representing the position in which the 2DST image is. (b) 2DST with a vertical line representing the time instant for the coronal image shown in (a). (c)-(d) Similar considerations for a sagittal image and its 2DST image.

by the breathing are present. Figs. 1(a)-(b) show a coronal image with its associated 2DST image. Figs. 1(c)-(d) show a sagittal image with its associated 2DST image.

The sagittal and the coronal images have a common vertical segment, and the pixels of such segment that are in the coronal and sagittal images occupy the same 3D position. Stevo et al. (2009) proposed an algorithm to determine the position of the vertical segments shown in Fig. 1(a) that is the intersection with the sagittal image shown in Fig. 1(c); and vice-versa. This way, the 2DST images shown in Figs. 1(b) and (d) represent the same vertical line in the 3D space over the time. Different temporal registration algorithms analyze these two 2DST images and for a given coronal image (see Fig. 1(a) and the vertical line in Fig. 1(b)) determines the time instant associated with the sagittal image that registers it; and vice-versa. The methods proposed for temporal registration can be classified into two groups: pixel intensity comparison (Stevo et al., 2009; Masuda and Haneishi, 2010), and diaphragmatic surface comparison (Sato et al., 2011).

This research uses the diaphragmatic surface to perform the temporal registration. The diaphragm has a movement with larger amplitude and a significant gradient. A standard respiratory function $f_s(t)$ (Matsushita et al., 2004), an estimation of the lung motion in an $I(x, y, t)$ is determined. The $f_s(t)$ is the input to a modified Hough transform proposed by Matsushita et al. (2004), to determine the presence of synchronous movement patterns $f_k(t)$ in vertical 2DST images. Since the lung movement is not totally synchronous, a greedy snake algorithm adapted
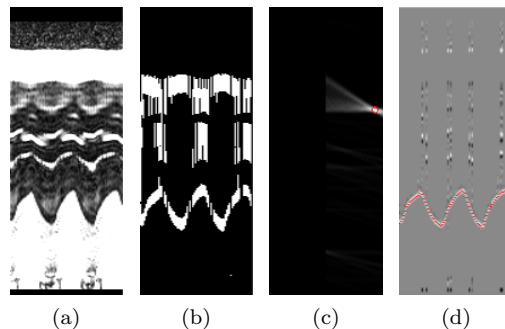

Fig. 2. (a) Original 2DST image. (b) 2DST image created from lung masks. (c) The parametric Hough space. (d) The original 2DST image filtered with lung masks and the determined diaphragmatic motion pattern.

by Kadota et al. (2005) relaxes the synchronicity restriction.

2.1 Diaphragmatic Motion Pattern Determination

The modified Hough transform determines several motion patterns in the 2DST image. Several authors (Sato et al., 2011; Stevo et al., 2012) manually determined the diaphragmatic motion pattern. Tavares et al. (2010) used lung masks to determine the diaphragmatic motion pattern using the Hough transform (see Fig. 2). Fig. 2(a) shows the original 2DST image. Fig. 2(b) shows a 2DST image create from the lung masks. Some masks were not correctly determined generally in the upper part of the lung. Near the diaphragm, the lung masks are correctly determined as consequence of the good contrast. The parametric Hough space is shown in Fig. 2(c), the pixel with higher intensity represents the diaphragmatic motion pattern. Fig. 2(d) shows the determined diaphragmatic motion pattern.

The diaphragmatic motion pattern is a specific motion pattern represented by $f_d(t)$. For a given time instant t_i, $f_d(t_i)$ outputs the diaphragmatic state

$$\{l, p\} = f_d(t_i)$$

where l represents the diaphragmatic level and p is the respiratory phase (inspiration or expiration).

The diaphragmatic motion pattern $f_d(t)$ can be determined from a temporal sequence of images A at the position in which the temporal sequence of images B crosses A. This is represented by

$$f_d(t) = \Gamma(A, B).$$

Considering the example shown in Fig. 1, the diaphragmatic motion pattern $f_d(t)$ present in Fig. 1(b) is obtained from a coronal temporal sequence A shown in Fig. 1(a) at the vertical that represents the position where the sagittal temporal sequence B crosses A (see Fig. 1(c)). Following the same logic, the diaphragmatic motion pattern present in Fig. 1(d) is obtained.

2.2 Temporal Registration

The temporal registration can be performed in different ways: Tsuzuki et al. (2009) compared lung silhouette's height, Masuda and Haneishi (2010) compared pixel by
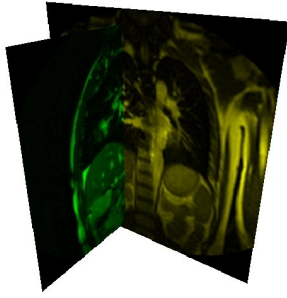
Fig. 3. Temporal registration between coronal and sagittal images.
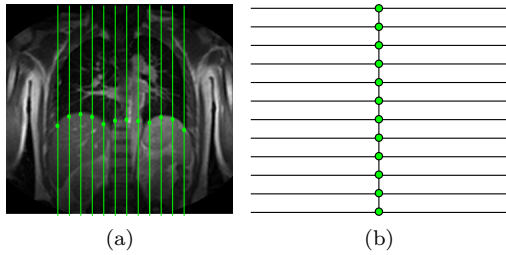

(a)   (b)

Fig. 4. (a) Original coronal image with the associated positions for sagittal temporal sequences. (b) Several temporal registrations (green circles) are executed with just one fixed coronal image (vertical) and several sagittal temporal sequences (horizontals).

pixel, and Sato et al. (2011) compared diaphragmatic motion patterns.

This work uses the temporal registration proposed by Sato et al. (2011). For a specific sagittal (coronal) image selected from a temporal sequence of images B, its diaphragmatic state (diaphragmatic level and respiratory phase) $f_d(t_B)$ is determined. Then a coronal (sagittal) image, from a temporal sequence of images A, with the same diaphragmatic state is determined. The determination is performed by comparing the diaphragmatic motion pattern $\Gamma(A, B)$. The temporal registration is represented by

$$\{t_i\} = \varrho(\Gamma(A, B), f_d(t_B))$$

where $\{t_i\}$ is the set of registered time instants. Fig. 3 shows an example of two registered coronal and sagittal images. It is possible to write the temporal registration as

$$\{t_i\} = \varrho(\Gamma(A, B), \Gamma(B, A)(t_B)),$$

this way it is clear the relation between the diaphragmatic motion patterns from both temporal sequences A and B.

2.3 Diaphragmatic Surface Reconstruction

By now, there are two different ways that the temporal registration can be used to reconstruct the diaphragmatic surface: *linear* and *cyclic* temporal registrations.

Linear Temporal Registration: uses one image as guide and several temporal registrations are performed with the orthogonal temporal sequences (see Fig. 4). Masuda and Haneishi (2010) used the linear registration with temporal registration based on pixel intensity comparison. Tsuzuki et al. (2009) used the linear registration with temporal registration based on lung height for temporal registration

to reconstruct the 3D animated lung using lung segmented silhouettes.

The linear temporal registration that uses the registration proposed by Sato et al. (2011) can be implemented by the following algorithm:

input : Coronal temporal sequence C_1
input : Sagittal temporal sequences S_i
input : Coronal image time instant $t_c^{c_1}$
output: $\{t_s^{s_i c_1}\}$: registration time instants.

begin
    for <*All sagittal temporal sequences S_i* > **do**
        $\{l_c, p_c\} = \Gamma(C_1, S_i)(t_c^{c_1})$;
        $\{t_s^{s_i c_1}\} = \varrho(\Gamma(S_i, C_1), \{l_c, p_c\})$;

Note that the set $\{t_s^{s_i c_1}\}$ can have more than one element, and it is not possible to decide which is better. When the set is empty, it is necessary to interpolate from adjacent silhouettes.

Cyclic Temporal Registration: four temporal sequences are given and a mesh temporal registration is performed to confirm the result. Consider the example shown in Fig. 5. Four temporal sequences are given in which two temporal sequences are sagittal S_1 and S_2 and the other two temporal sequences are coronal C_1 and C_2. The four temporal sequences cross each other at points A, B, C and D. One image from C_1 is considered fixed. The cyclic temporal registration searches for time instants that can coherently register simultaneously at all the four crossing points.

Similarly, the cyclic temporal registration that uses the registration proposed by Sato et al. (2011) can be implemented by the algorithm shown in Fig. 6 (see Fig. 5 for point references).

In this algorithm, after performing the temporal registration at points A and B, two sets of registered time instants are determined (sets $\{t_s^{s_1 c_1}\}$ and $\{t_s^{s_2 c_1}\}$). The temporal registration at points C and D are secondary registrations that use the previously determined results. Thus, it is necessary to associate the secondary registration with the time instant used from the primary registration. This is represented by sets of pair instants ($\{(t_c^{c_2 s_1}, t_s^{s_1 c_1})\}$ and $\{(t_c^{c_2 s_2}, t_s^{s_2 c_1})\}$). Operator $\star$ is used to create the correspondence between secondary and primary registrations. The
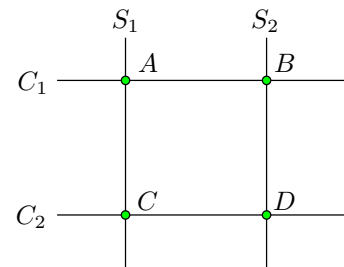

Fig. 5. Cyclic registration starting from just one fixed coronal image C_1. The temporal registration happens at A and B positions. Then, temporal registration happens at C and D. A confirmation if the same image C_2 can register in C and in D happens.

input : Coronal temporal sequences C_1 and C_2
input : Sagittal temporal sequences S_1 and S_2
input : Coronal image time instant $t_c^{c_1}$
output: $\{t_s^{s_1}\}$, $\{t_s^{s_2}\}$: registration time for S_1 and S_2
output: $\{t_c^{c_2}\}$: registration time for C_2
begin

    Registration for Point A;
    $\{t_s^{s_1 c_1}\} = \varrho(\Gamma(S_1, C_1), \Gamma(C_1, S_1)(t_c^{c_1}));$

    Registration for Point B;
    $\{t_s^{s_2 c_1}\} = \varrho(\Gamma(S_2, C_1), \Gamma(C_1, S_2)(t_c^{c_1}));$

    Registration for Point C;
    $\{t_c^{c_2 s_1}\} = \{(t_1^{c_2 s_1}, t_s^{s_1 c_1})\} = \oslash;$
    for $<$All $t_i \in \{t_s^{s_1 c_1}\} >$ **do**
        $\alpha = \varrho(\Gamma(C_2, S_1), \Gamma(S_1, C_2)(t_i));$
        $\{t_c^{c_2 s_1}\} = \{t_c^{c_2 s_1}\} \bigcup \alpha;$
        $\{(t_c^{c_2 s_1}, t_s^{s_1 c_1})\} = \{(t_c^{c_2 s_1}, t_s^{s_1 c_1})\} \bigcup \{\alpha \star t_i\};$

    Registration for Point D;
    $\{t_c^{c_2 s_2}\} = \{(t_2^{c_2 s_2}, t_s^{s_2 c_1})\} = \oslash;$
    for $<$All $t_j \in \{t_s^{s_2 c_1}\} >$ **do**
        $\beta = \varrho(\Gamma(C_2, S_2), \Gamma(S_2, C_2)(t_j));$
        $\{t_c^{c_2 s_2}\} = \{t_c^{c_2 s_2}\} \bigcup \beta;$
        $\{(t_c^{c_2 s_2}, t_s^{s_2 c_1})\} = \{(t_c^{c_2 s_2}, t_s^{s_2 c_1})\} \bigcup \{\beta \star t_j\};$

    Check Validity;
    if $< \{t_c^{c_2 s_1}\} \bigcap \{t_c^{c_2 s_2}\} \neq \oslash >$ **then**
        $\{t_c^{c_2}\} = \{t_c^{c_2 s_1}\} \bigcap \{t_c^{c_2 s_2}\};$
        $\{t_s^{s_1}\} = \text{filter}(\{(t_c^{c_2 s_1}, t_s^{s_1 c_1})\}, \{t_c^{c_2}\} >;$
        $\{t_s^{s_2}\} = \text{filter}(\{(t_c^{c_2 s_2}, t_s^{s_2 c_1})\}, \{t_c^{c_2}\} >;$
    else
        $\{t_c^{c_2}\} = \{t_s^{s_1}\} = \{t_s^{s_2}\} = \oslash;$

Fig. 6. Algorithm for the cyclic temporal registration.

obtained temporal registrations for C_2 are filtered such that the same time instant can register at both positions C and D. The final sets of instant registrations are $\{t_c^{c_2}\}$, $\{t_s^{s_1}\}$ and $\{t_s^{s_2}\}$.

While it gives a reliable set of temporal registrations, the amount of results found is reduced. Stevo et al. (2010) observed that the cyclic registration is not always possible.

3. METHOD PROPOSED

The method proposed combines the linear temporal registration simplicity with the cyclic temporal registration reliability. It is divided in three steps: massive temporal registration, registration validation and diaphragmatic surface reconstruction.

3.1 Massive Temporal Registration

The temporal registration is performed for all coronal-sagittal intersections. The algorithm is shown in Fig. 7. Additional details about the algorithm flow are shown in Fig. 8. Initially, a coronal image (time instant $t_c^{c_1}$) is defined as root. The first loop represents the algorithm first level in which the temporal registration is performed with all crossing sagittal temporal sequences. The blue squares shown in Fig. 9(a) represent the positions where the coronal image diaphragmatic state was determined. The green squares represent that the temporal registration was

input : Coronal temporal sequences C_j
input : Sagittal temporal sequences S_i
input : Root coronal image time instant $t_c^{c_1}$
output: $\{t_s^{s_i c_1}\}$: registration time for S_i
output: $\{(t_c^{c_j s_i}, t_s^{s_i c_1})\}$: registration time for C_j
begin

    Registration for first level;
    for $<$All sagittal temporal sequences $S_i >$ **do**
        $\{t_s^{s_i c_1}\} = \varrho(\Gamma(S_i, C_1), \Gamma(C_1, S_i)(t_c^{c_1}));$

        Registration for second level;
        for $<$All coronal temporal sequences $C_j >$ **do**
            $\{t_c^{c_j s_i}\} = \{(t_c^{c_j s_i}, t_s^{s_i c_1})\} = \oslash;$
            for $<$All $t_i \in \{t_s^{s_i c_1}\} >$ **do**
                $\gamma = \varrho(\Gamma(C_j, S_i), \Gamma(S_i, C_j)(t_i));$
                $\{t_c^{c_j s_i}\} = \{t_c^{c_j s_i}\} \bigcup \gamma;$
                $\{(t_c^{c_j s_i}, t_s^{s_i c_1})\} = \{(t_c^{c_j s_i}, t_s^{s_i c_1})\} \bigcup \{\gamma \star t_i\};$
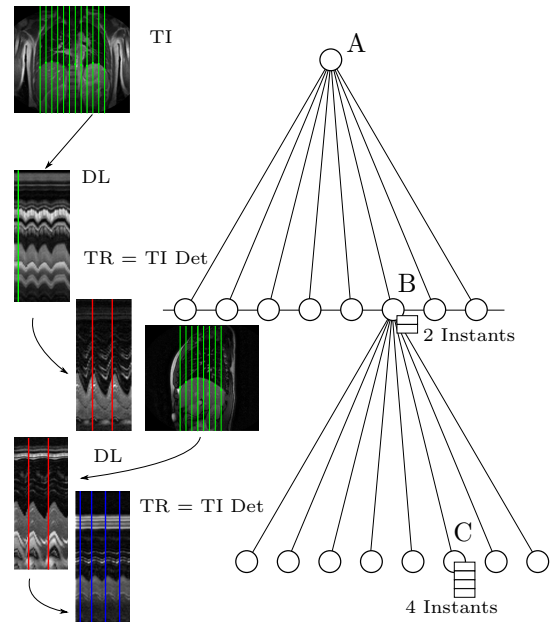
Fig. 7. Massive temporal registration algorithm.

Fig. 8. Massive temporal registration algorithm flow. TI = Time Instant; DL = Diphragmatic Level Determination; TR = Temporal Registration; TI Det = Time Instant Determination.

successful with at least one sagittal time instant $\{t_s^{s_i c_1}\}$. The white squares represent that no temporal registration was possible.

The second and third loops in the massive temporal registration algorithm (see Fig. 7), perform the second level temporal registration. All the coronal temporal sequences (except the root) are temporal registered considering the temporal registrations determined in the first level. Fig. 9(b) shows red squares representing positions where the temporal registration was possible in the second level. The yellow squares represent positions where the diaphragmatic level was determined as a consequence of the second level temporal registration.
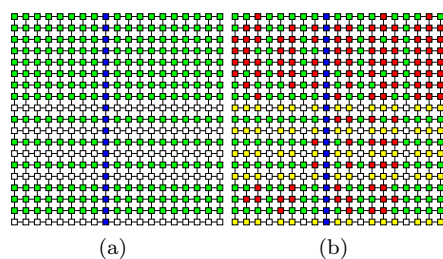
(a)   (b)

Fig. 9. (a) Squares represent positions where the diaphragmatic level can be determined (algorithm first level): blue (from root image), green (from first level registration), and white (no registration in the first level). (b) Red squares represent where the second level temporal registration was possible. Yellow squares represent where the diaphragmatic level was determined (algorithm second level).
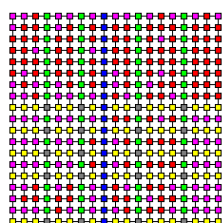

Fig. 10. Blue and red squares represent locally consistent diaphragmatic levels. Green and yellow squares represent locally inconsistent diaphragmatic level with global consistency. Purple squares represent inconsistent diaphragmatic levels. Gray squares represent positions where the diaphragmatic level can not be defined, requiring interpolation with adjacent positions.

3.2 Registration Validation and Surface Reconstruction

The temporal registration was executed massively. Now, it is necessary to filter the results and eliminate inconsistencies, similar to the process performed by the cyclic temporal registration. Two types of consistency can be observed here: local consistency by analyzing the two crossing temporal sequences, and global consistency in which the all temporal registrations originated from one temporal sequences are simultaneously analyzed.

Locally consistent diaphragmatic levels are represented by colors blue, red, green and yellow in Fig. 10: blue squares are associated with the original coronal root image, red squares are associated to positions where second level temporal registration was possible, green and yellow squares represent positions where the diaphragmatic level was determined exclusively from, respectively, sagittal and coronal temporal sequences. Purple squares represent inconsistent diaphragmatic levels in which a temporal registration was not possible. However, coronal and sagittal temporal sequences determine distinct diaphragmatic levels. Gray squares represent positions where the diaphragmatic level was not possible to be determined.

It is possible to observe that several cyclic temporal registrations are present, but they are minority when compared to all other cases. The global consistency states that all the diaphragmatic levels associated to the same image must be represented by the same time instant. This

(a)   (b)   (c)
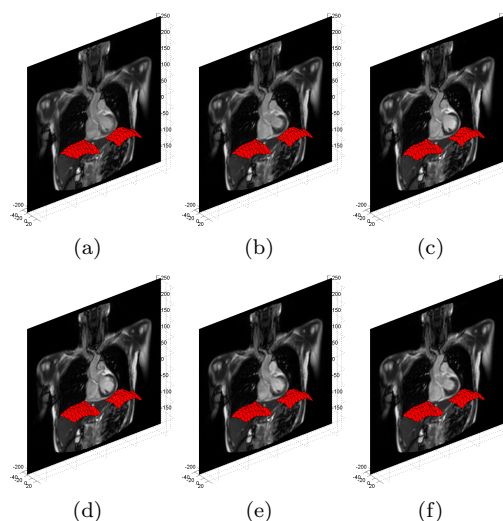
(d)   (e)   (f)

Fig. 11. Diaphragmatic surface reconstructed in movement.

way, the sagittal time instants for each horizontal must be just one. The same is true for the verticals representing coronal images.

All sagittal (horizontal) and coronal (vertical) temporal sequences are analyzed to determine the time instant that majority appears. This procedure will keep global consistency. Verticals with green squares and horizontals with yellow squares are not considered (see Fig. 10) as they do not have diaphragmatic levels originated, respectively, from coronal and sagittal temporal sequences. To remove local inconsistencies (purple squares shown in Fig. 10), the diaphragmatic level is defined as the average between crossing sagittal and coronal temporal sequences. The complete procedure was explained with a coronal image as root, and exactly the same procedure happens if the root is a sagittal image instead.

The diaphragmatic level associated with the gray squares is determined by interpolation among adjacent diaphragmatic levels.

With all diaphragmatic levels determined, the diaphragmatic surface is reconstructed by creating triangles with adjacent nodes. These three steps are repeated for each image in the temporal sequence associated with the root node, creating several frames to compose the animated model.

4. RESULTS

The MR image sequences used in the experiment were obtained by Symphony (1.5T) made by Siemens, using True-FISP. MR images were obtained from one healthy nonsmoker [10] . Initial images in dynamic data sets were acquired in the transient state of magnetization, so they have high signal intensity and different contrast. The analysis included all acquired images, including the initial images. It was acquired 28 temporal sequences, 5 coronal and 23 sagittal. Fig. 11 shows a reconstructed diaphragmatic surface.

---

[10] The protocol was approved by the hospital medical-ethics committee of Kanagawa Cardiovascular Respiratory Center, and informed consent was obtained from the patient.
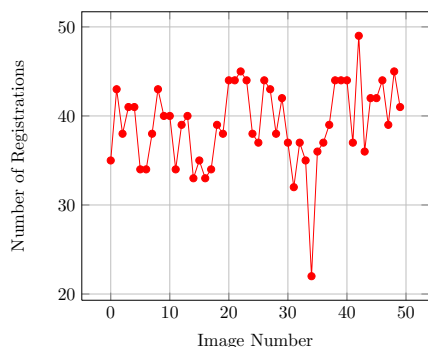
Fig. 12. Number of complete registrations in the final configuration at each image in a temporal sequence.

Figure 12 shows at each time instant (image in a temporal sequence) the number of consistent temporal registrations. Considering that the total number of temporal registrations is 95, then averagely 41% are consistent registrations. This is a consequence of the fact that the breathing range was different for each temporal sequence. Fig. 13 shows the average displacement to place the diaphragmatic level correctly where consistent temporal registration was not possible. This research used data from a single health subject and more data from other subjects is necessary for intra-individual variability considerations.

5. CONCLUSION AND FUTURE WORKS

The proposed method showed to reconstruct the diaphragmatic surface with higher confidence, when compared to previously published methods, as redundant information was used. It combines the linear and cyclic temporal registrations. All possible temporal registrations between sagittal and coronal sequences are determined, and data coherence is kept by analyzing global and local consistencies.

This is a preliminary work, and several further evaluations are necessary. The registration of the reconstruct diaphragmatic surface with a 3D lung CT image can be used to evaluate the proposed method error. By determining the minimum number of temporal sequences necessary to reconstruct the diaphragmatic surface, it will be possible to reduce the time inside the MR device.
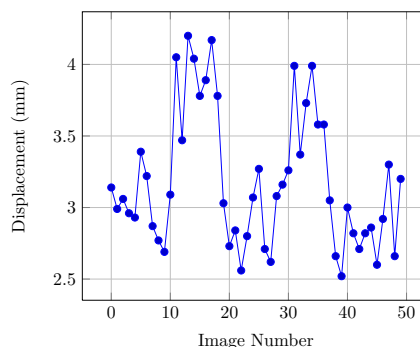
6. ACKNOWLEDGEMENTS

Fig. 13. Average displacements at each image in a temporal sequence.

analysis with automated lung field tracking in MRI temporal sequences. In *Proc 18th IFAC WC*, 5001–5006.

REFERENCES

Cluzel, P, Similowski, T, Chartrand-Lefebvre, C, Zelter, M, Derenne, JP, and Grenier, PA (2000). Diaphragm and chest wall: assessment of the inspiratory pump with MR imaging–preliminary observations. *Radiol*, 215, 574–583.

Gotoh, T, Hosoda, Y, Yanagita, T, Kagei, S, Iwasawa, T, Inoue, T, and Tsuzuki, MSG (2011). Motion complexity

Iwasawa, T, Kagei, S, Gotoh, T, Yoshiike, Y, Matsushita, K, Kurihara, H, Saito, K, and Matsubara, S (2002). Magnetic resonance analysis of abonormal diaphragmatic motion in patients with emphysema. *Eur Respir J*, 19, 225–331.

Kadota, E, Gotoh, T, Kagei, S, and Iwasawa, T (2005). Shape tracking and motion pattern analysis on chest mr sequence images using respiratory and heartbeat patterns. *IEICE Tech Rep*, 105, 9–12.

Masuda, Y and Haneishi, H (2010). 4D MR imaging of respiratory organ motion using an intersection profile method. In *Proc SPIE Medical Imaging*. San Diego, USA.

Matsushita, K, Asakura, A, Kagei, S, Gotoh, T, Iwasawa, T, and Inoue, T (2004). Shape tracking on chest MR sequence images using respiratory patterns. *JIIEEJ*, 33, 1115–1122.

Sato, AK, Stevo, N, Tsuzuki, MSG, Kadota, E, Gotoh, T, Kagei, S, and Iwasawa, T (2011). Registration of temporal sequences of coronal and sagittal MR images through respiratory patterns. *Biomed Signal Proces*, 6, 34–47.

Stevo, N, Gotoh, T, Kagei, S, Iwasawa, T, and Tsuzuki, MSG (2012). Animated 3D lung surface reconstruction from asynchronous MR image sequences based on multiple registration. In *Proc 5th BMEI*, 153–157. Chongqing, China.

Stevo, N, Campos, R, Tavares, RS, Tsuzuki, MSG, Gotoh, T, Kagei, S, and Iwasawa, T (2009). Registration of temporal sequences of coronal and sagittal images obtained from magnetic resonance. In *Proc COBEM 2009*. Gramado, Brazil.

Stevo, N, Sato, AK, Tsuzuki, MSG, Gotoh, T, Kagei, S, and Iwasawa, T (2010). Multiple registration of coronal and sagittal MR temporal image sequences based on Hough transform. In *Proc 32nd IEEE EMBS*. 5943–5946, Buenos Aires, Argentina.

Tavares, RS, Sato, AK, Tsuzuki, MSG, Gotoh, T, Kagei, S, Asakura, A, and Iwasawa, T (2010). Temporal segmentation of lung region MR images sequences using Hough transform. In *Proc 32nd IEEE EMBS*. 4789–4792, Buenos Aires, Argentina.

Tsuzuki, MSG, Takase, FK, Gotoh, T, Kagei, S, Asakura, A, Iwasawa, T, and Inoue, T (2009). Animated solid model of the lung constructed from unsynchronized MR sequential images. *CAD*, 41, 573–585.